HHS Public Access

Author manuscript

J Bone Miner Res. Author manuscript; available in PMC 2020 October 01.

Published in final edited form as:

J Bone Miner Res. 2019 October ; 34(10): 1910–1922. doi:10.1002/jbmr.3763.

Novel Role for Claudin-11 in the Regulation of Osteoblasts via Modulation of ADAM10-mediated Notch Signaling

Richard C. Lindsey[1,2,3], **Weirong Xing**[1,4], **Sheila Pourteymoor**[1], **Catrina Godwin**[1], **Alexander Gow**[5,6,7], **Subburaman Mohan**[1,2,3,4,8]

[1]Musculoskeletal Disease Center, VA Loma Linda Healthcare System, Loma Linda, CA, USA

[2]Center for Health Disparities and Molecular Medicine, School of Medicine, Loma Linda University, Loma Linda, CA, USA

[3]Division of Biochemistry, Department of Basic Sciences, School of Medicine, Loma Linda University, Loma Linda, CA, USA

[4]Department of Medicine, School of Medicine, Loma Linda University, Loma Linda, CA, USA

[5]Center for Molecular Medicine and Genetics, Wayne State University, Detroit, MI, USA

[6]Carman and Ann Adams Department of Pediatrics, Wayne State University, Detroit, MI, USA

[7]Department of Neurology, Wayne State University, Detroit, MI, USA

[8]Department of Orthopedics, School of Medicine, Loma Linda University, Loma Linda, CA, USA

Abstract

The claudin (Cldn) family comprises 27 members of 20–34 kDa transmembrane tight junction proteins. In addition to their established canonical role as barriers controlling paracellular flow of molecules, a distinct non-canonical role for Cldns as mediators of cell signaling is now emerging. In our studies evaluating Cldn family expression levels during osteoblast differentiation, *Cldn-11* showed the largest increase (60-fold). Immunohistochemistry studies revealed high Cldn-11 expression in trabecular (Tb) bone lining cells. MicroCT analysis of femurs, tibiae, and vertebrae of Cldn-11 knockout (KO) mice at 12 weeks of age exhibited a 40% ($P < 0.01$) reduction in Tb bone volume adjusted for tissue volume compared to control mice, a change caused by significant reductions in Tb number and thickness and increase in Tb separation. Histomorphometry and serum biomarker studies revealed that reduced bone formation, not increased resorption, is the cause for reduced Tb bone volume in the Cldn-11 KO mice. Cldn-11 KO osteoblasts expressed reduced *ALP* and *BSP* while *Cldn-11* overexpression in MC3T3-E1 cells increased expression of *ALP* and *BSP*. Mechanistically, Cldn-11 interacted with tetraspanin (Tspan)3 in osteoblasts, and *Tspan3* knockdown reduced osteoblast differentiation. Since members of the Tspan family regulate cell functions via Notch signaling, we evaluated whether Cldn-11/Tspan3 regulates Notch signaling in osteoblasts. Accordingly, Notch targets *Hey1* and *Hey2* were significantly upregulated in *Cldn-11* overexpressing cultures but downregulated in both *Cldn-11* KO and *Tspan3* knockdown osteoblasts. Since ADAM10 has been shown to interact with Tspan family members

Corresponding author: Subburaman Mohan, Ph.D., Musculoskeletal Disease Center (151), 11201 Benton St., Loma Linda, CA 92357, Tel: +1 (909) 825-7084 × 6180, Fax: +1 (909) 796-1680, subburaman.mohan@va.gov.

to regulate Notch signaling, we evaluated whether Cldn-11 regulates ADAM10 expression. Cldn-11 overexpressing cells express more mature ADAM10, and an ADAM10 inhibitor blocked the Cldn-11 effect on osteoblast differentiation. Based on these data, we propose Cldn-11 as a novel component of a osteoblast cell surface protein complex, comprising Tspan3 and ADAM10, which regulates Notch signaling and cell differentiation.

Keywords

Tight junctions; claudin-11; osteoblasts; ADAM10; Notch

Introduction

Osteoporosis is the most common significant age-related public health problem affecting over 10 million people in the U.S. alone. The pathogenesis of postmenopausal and senile osteoporosis involves an increase in bone resorption that is not compensated by a corresponding increase in bone resorption, resulting in net bone loss.[1] Therefore, a more complete understanding of molecular pathways that regulate the formation and activity of osteoblasts is important in identifying defective pathways in osteoporotic individuals and in developing optimal strategies for the treatment of osteoporosis. In our effort to identify novel regulatory molecules that control osteoblast development, we focused on claudins (Cldns), the principle proteins responsible for the formation of tight junction strands.[2,3] The Cldn family of proteins comprises 27 members with molecular weights ranging from 20–34 kDa. Cldns are divided into two major groups based on their sequence and functional properties: “classic” and “non-classic” claudins.[4] Moreover, Cldns exhibit complex patterns of expression that are specific to tissue/cell type and developmental stage.[5,6] As for their function, Cldns act canonically as barriers/pores that regulate paracellular permeability to ions and small molecules, serving as a fence that divides the apical and basolateral domains of plasma membranes.[2-4] Recently, a distinct non-canonical role for Cldns has emerged in which they serve as mediators of cell signaling, controlling cell proliferation and differentiation.[6,7]

Functional roles for several Cldn family members have been identified by loss-of-function studies in mice. Deletion of Cldn-11 hampers CNS saltatory nerve conduction, induces behavioral phenotypes and neurotransmitter imbalances, and causes male sterility.[8-11] Ablation of Cldn-14, Cldn-1, and Cldn-5 affect cochlear hair cell function, the skin, and blood–brain barriers, respectively.[12-14] A severe renal phenotype is observed in mice lacking Cldn-7, Cldn-16, or Cldn-19, while mice deficient in Cldn-15 exhibit megaintestine.[15-18] Until recently, the role of Cldns in bone had not been investigated. Our recent studies showed for the first time that osteoclasts express Cldn-18 and that its deletion in mice results in an osteopenia phenotype. Interestingly, loss of Cldn-18 function in the skeleton was found to be independent of tight junction function and was instead mediated by increased bone resorption and osteoclast differentiation.[19-21] In addition to our previously published studies providing the foundation for the non-canonical function of Cldn-18 involving modulation of RANKL signaling in regulating bone homeostasis[19-21] and Cldn-1 as a positive regulator of osteoblastogenesis,[22] a recent study has indicated a possible role for

Cldn-11 in osteoblast and osteoclast function mediated via bidirectional EphB4–EphrinB2 signaling.[23]

In this study, we focused on elucidating the role and mechanism of action of Cldn-11 in osteoblasts as we had previously reported that this Cldn was found to be highly regulated during differentiation of osteoblasts.[22] In addition to osteoblasts, Cldn-11 is also expressed at high levels in articular chondrocytes. Therefore, we evaluated the consequence of targeted disruption of the *Cldn-11* gene on the bone and cartilage phenotypes in mice. Our findings demonstrate that Cldn-11 is an important regulator of osteoblast and chondrocyte functions that acts non-canonically by interacting with tetraspanin-3 to modulate ADAM10-mediated Notch signaling.

Materials and Methods

Mice

C57BL/6J mice were obtained from The Jackson Laboratory (Bar Harbor, ME, USA). Mice deficient in Cldn-11 (*Cldn-11*$^{-/-}$) were generated by replacing the coding region of exon 1 and 0.3 kb of the 5′ end of intron 1 with the lacZ coding sequence and a floxed PGKneo cassette by homologous recombination in 129SvEvBrd-derived embryonic stem (ES) cells as described.[8] Histochemical staining of β-galactosidase activity in embryos using X-gal was performed as previously reported.[8] Embryos were rendered transparent by 20 minute incubations in ethanol and a 1:1 mixture of benzyl benzoate:benzyl alcohol at room temperature.[9] Genotyping of mice was accomplished using WT- and mutant-specific primers (Supplemental Table 1) for PCR. Littermate controls were used for all experiments. Mice were group housed at the Veterinary Medical Unit of the VA Loma Linda Healthcare System (Loma Linda, CA) under standard approved, pathogen-free laboratory conditions and fed *ad libitum* with Teklad 4% Fat Mouse/Rat Diet (7001, Harlan Laboratories, Madison, WI, USA). Animal use protocols were approved by the Institutional Animal Care and Use Committee of the participating institutions.

Cell culture

Primary calvarial osteoblasts and bone marrow macrophages were obtained from newborn C57BL/6J mice or Cldn-11 KO mice and their littermate controls as previously described.[24,25] Briefly, calvariae were isolated via enzymatic digestion with collagenase I (2 mg/mL) and hyaluronidase (1 mg/mL), and bone marrow macrophages were isolated by flushing the marrow of femurs and tibiae and discarding cells which initially adhere to culture plates. Cells were maintained in ascorbic acid (AA)-free alpha-MEM growth medium supplemented with 10% fetal bovine serum, penicillin (100 units/mL), and streptomycin (100 μg/mL). Osteoblast differentiation was induced by treatment with 50 μg/mL AA in the presence of 10 mM β-glycerophosphate (unless other treatment concentrations are specified). Osteoclast differentiation was induced by incubating non-adherent bone marrow macrophages with MCSF (25 ng/mL) and RANKL (50 ng/mL; both obtained from R&D Systems, Minneapolis, MN, USA) for six days.

Micro-computed tomography

The trabecular bone phenotype of 12-week-old *Cldn-11*$^{-/-}$ mice and their control littermates of both genders was evaluated at the distal femur and fifth lumbar vertebra via micro-computed tomography (microCT, Scanco vivaCT 40, Scanco Medical, Bruttisellen, Switzerland). For femur, the trabecular region of interest started 0.36 mm from the distal growth plate in the direction of the metaphysis and extended for 2.25 mm. For vertebra L5, the entire trabecular bone within the vertebral body was analyzed. The bones were scanned at a resolution of 10.5 μm with a 55 kVp X-ray for measurement of trabecular bone microstructure. Cortical bone was scanned at 10.5 μm resolution, 70 kV energy, and 114 μA intensity. All images were reconstructed and analyzed by Scanco software as described previously.[26] Parameters included trabecular bone volume fraction (BV/TV), trabecular number (Tb.N, mm^{-1}), trabecular thickness (Tb.Th, mm), trabecular separation (Tb.Sp, mm), and connectivity density (Conn.D, mm^{-3}). Nomenclature of all microCT data follows guidelines of the American Society for Bone and Mineral Research.[27]

Histology and histomorphometry

For TRAP staining, bones were fixed in formalin, decalcified in EDTA, and embedded in paraffin before being sectioned at 5 μm and stained according to standard procedures. For static histomorphometry, bones were fixed, dehydrated in alcohol, and infiltrated with methyl methacrylate. After sectioning, osteoid was stained using Goldner's trichrome method. Osteoid was quantitated by a blinded observer using the OsteoMeasure system (OsteoMetrics, Atlanta, GA, USA). Articular cartilage was stained with Safranin-O.

Immunohistochemistry (IHC)

Paraffin-embedded tissues were sectioned for IHC. Consecutive tissue sections were deparaffinized in HistoChoice clearing agent (Sigma-Aldrich, St. Louis, MO, USA), rehydrated in a graded series of ethanol and tap water solutions, and treated with 3% H_2O_2 for 30 minutes to inactivate endogenous peroxidase activity. The sections were then rinsed thoroughly with PBS (pH 7.4) and incubated in 2 mg/mL hyaluronidase (pH 7.4; Sigma-Aldrich) for 30 minutes at 37°C for epitope recovery. Each section was pretreated with a blocking solution containing normal goat serum for 20 minutes before incubation with primary antibodies for Cldn-11 or Tspan3 (both diluted 1:100; Cldn-11 and Tspan3 antibodies were kindly provided by Dr. Jeff Bronstein, University of California at Los Angeles) or with antibodies for lubricin (ab28484, Abcam, Cambridge, UK) or collagen 10 (ab58632, Abcam). After an overnight incubation at 4°C, the sections were rinsed with PBS and incubated with secondary antibodies. Colorimetric IHC images were prepared with a Vectastain ABC Kit (Vector Laboratories, Burlingame, CA, USA).

Serum alkaline phosphatase (ALP) and tartrate-resistant acid phosphatase (TRAP) assays

Serum was collected from Cldn-11 KO and control mice, diluted (1:10 for TRAP and 1:100 for ALP), and added to wells of a 96-well plate. To measure phosphatase activity, a solution containing p-nitrophenyl phosphate (PNPP) substrate was added. For ALP assays, absorbance was read in a plate reader at intervals 0-, 1-, 3-, and 5-hour time points. For TRAP assays, plates were incubated with substrate in a solution containing 80 mM sodium

tartrate at 37°C for 30 minutes before stopping the reaction with 1 M NaOH, and absorbance was then read in a plate reader. The difference in absorbance at 490 nm and 410 nm was used to calculate enzyme activity over time, which was normalized to total protein concentration as measured by a Pierce™ BCA kit according to manufacturer's instructions (ThermoFisher Scientific, Waltham, MA, USA).

Immunoblotting

Cells were lysed in a buffer containing 0.5% SDS, 0.1% v/v Triton X-100, 0.25% sodium deoxycholate, 12.5 mM tris, 96 mM glycine (pH 8.3), 1 mM DTT, and 1× protease inhibitor cocktail (Sigma-Aldrich). Lysate protein concentrations were determined with a Bradford assay, and equal amounts of protein were run on SDS-PAGE gels for immunoblotting on PVDF membranes. Membranes were probed with antibodies specific for Cldn-11, Tspan3, mature ADAM10 (ab124695, Abcam, Cambridge, UK), NICD1 (anti-activated Notch1, ab8925, Abcam), and β-actin (A5441, Sigma-Aldrich, St. Louis, MO, USA) followed by secondary antibody incubation, chemiluminescent imaging, and quantitation with ImageJ.

Immunoprecipitation

Cells were incubated in lysis buffer containing 50 mM Tris-HCl (pH 7.4), 150 mM NaCl, 1% NP-40, 1 mM DTT, and 1× protease inhibitor cocktail for 30 minutes on ice followed by centrifugation at 12,000 x *g* for 10 minutes. Immunoprecipitation was performed by incubating lysate with Tspan3 antibody, Cldn-11 antibody, or isotype control rabbit immunoglobulin G (IgG, 2729, Cell Signaling Technology, Danvers, MA, USA) at room temperature for one hour as described.[28] The immunoprecipitated proteins were separated by SDS-PAGE under reducing conditions for immunoblotting and probed with antibody against Cldn-11 or Fluor-488 conjugated Tspan3 antibody.

Overexpression

The lentiviral pRRLsin-cPPT-SSFV-*Cldn-11*-wpre plasmid was generated by replacing GFP with a PCR product of mouse *Cldn-11* using the *Sgf1* and *Pmel* restriction sites of the pRRLsin-cPPT-SSFV-GFP-wpre vector. Lentiviral particles were generated by co-transfection of pRRLsin-cPPT-SSFV-*Cldn-11*-wpre plasmid or pRRLsin-cPPT-SSFV-GFP-wpre control plasmid with Pax2 and VSVG plasmids in 293T cells as described previously.[29] Forty-eight hours after transfection with FuGene, culture supernatants containing viral particles were collected, spun at 2,000 × g for 10 minutes, and filtered through a 0.45 mm filter. Titers were determined by infecting 293T cells with serial dilutions and examining GFP expression of infected cells 24 hours after infection. MC3T3-E1 pre-osteoblasts and ATDC5 chondrocytes were transduced by adding Lenti-GFP or Lenti-Cldn-11 viral supernatant at a multiplicity of infection (MOI) of 5 in the presence of polybrene (8 μg/mL) for 24 hours followed by replacement of fresh DMEM/F12 medium containing 10% FBS, penicillin (100 units/mL), and streptomycin (100 μg/mL).

Alizarin Red staining

Cldn-11 or GFP overexpressing MC3T3-E1 cells were allowed to grow in culture in αMEM containing 10% calf serum for 23 days before staining with Alizarin Red S (A5533, Sigma-Aldrich). Images were quantitated with ImageJ.

shRNA knockdown

MC3T3-E1 cells were transduced with control or Tspan3 Mission lentiviral shRNA particles (Sigma-Aldrich, St. Louis, MO, USA) and selected with puromycin before induction of differentiation with AA and β-glycerophosphate as described.[30]

Gene expression analysis

Total RNA was extracted from isolated tissues or cells for cDNA synthesis and real time RT-PCR analysis as previously described.[31] Relative gene expression levels were examined and normalized to expression of the housekeeping gene PPIA. The fold-change compared to control was calculated according to the formula $2^{-\Delta\Delta Ct}$. Primer sequences are listed in Supplemental Table 2.

Statistical analysis

Results are expressed as mean ± SEM. *Cldn-11* and *ALP* mRNA expression level time courses (Fig. 1C) were each analyzed using a one-way ANOVA followed by Newman-Keuls post-hoc tests (GraphPad Prism6). All other experiments were analyzed using Student's *t*-tests (Microsoft Excel). Differences were considered significant when $P < 0.05$.

Results

Regulation of Cldn-11 expression in bone cells

Studies on regulation of Cldn expression in other tissues have shown that this protein family exhibits complex patterns of expression in multiple tissues and cell types as well as developmental stages. For example, Cldn-11 is broadly expressed in embryonic day 14.5 embryos, including in long bones such as ribs and the sternum (Fig. 1A). To determine if Cldn-11 is expressed in bone cells *in vivo*, we performed immunostaining with anti-Cldn-11 in paraffin sections prepared from 12-week old WT mice. Fig. 1B shows that Cldn-11 is highly expressed in lining cells of trabecular bone, consistent with our previous report.[22] We also observed some Cldn-11 expression in osteocytes and marrow cells. In order to determine if *Cldn-11* expression is regulated during osteoblast differentiation, primary calvarial osteoblasts isolated from 3-day-old C57BL/6J mice were cultured to confluence and induced to differentiate by the addition of 100 μg/mL of ascorbic acid (AA). At different time points (0, 4, 6, 8, 13, 19, and 24 days), RNA was extracted and used for real time RT-PCR. Fig. 1C shows *Cldn-11* expression is increased rapidly during early phases of osteoblast differentiation, with a 60-fold increase at day 8 compared to day 0, and then declined during late stages of osteoblast differentiation. The increase in *Cldn-11* expression preceded the increase in alkaline phosphatase (*ALP*) mRNA levels. In order to determine if Cldn expression patterns during osteoclast differentiation are similar to or different from the patterns observed in osteoblasts, we induced differentiation of osteoclast precursors derived

from long bones of C57BL/6J mice by adding MCSF (25 ng/mL) and RANKL (50 ng/mL). Cldn mRNA levels were measured at day 0, 1, and 6 after treatment. Interestingly, consistent with a recent report,[23] *Cldn-11* expression decreased by 75% and 50%, respectively, at day 1 and day 6 after treatment with MCSF and RANKL (Fig. 1D). These data show that regulation of *Cldn-11* expression patterns is cell type- and differentiation stage-dependent. It is known that osteoblast differentiation is subject to regulation by systemic factors in addition to autocrine/paracrine factors produced locally within the bone microenvironment. To determine if expression of *Cldn-11* is subject to regulation by systemic and local factors, we evaluated the effects of AA, BMP7, Wnt3a, and $1,25(OH)_2D_3$ on *Cldn-11* mRNA levels 24 hours after treatment using serum-free cultures of osteoblasts derived from calvariae of 3-day-old mice. Besides AA, BMP7 and $1,25(OH)_2D_3$ increased expression of *Cldn-11* mRNA. However, Wnt3a decreased *Cldn-11* expression (Fig. 1E). In order to determine the translational value of these findings to humans, we evaluated the effects of AA and BMP7 on *Cldn-11* mRNA levels in untransformed normal human osteoblasts derived from rib. We found that both AA and BMP7 caused a significant increase in *Cldn-11* expression in normal human osteoblasts (Fig. 1F), thus suggesting the relevance of findings obtained in mouse osteoblasts to humans.

Skeletal phenotype of Cldn-11 KO mice

In order to determine whether a lack of Cldn-11 influences the skeletal phenotype, microCT analyses of the femurs, tibias, and vertebrae of Cldn-11 KO mice were performed using the vivaCT40 scanner. Fig. 2A shows representative microCT images of the distal femur of 12-week-old female WT and KO mice. Consistent with the reduced trabecular bone volume (BV) in the Cldn-11 KO mice as seen in the images, quantitative analyses revealed that trabecular BV adjusted for tissue volume (TV) was reduced by 40% in the KO mice compared to littermate control mice (Fig. 2B). The decrease in trabecular BV in the KO mice is caused by a significant decrease in trabecular number and thickness and an increase in trabecular separation. The loss of trabecular elements reduced the number of interconnections between trabeculae as reflected by a > 40% reduction in connectivity density in the KO mice (Fig. 2C-F). Similar trabecular changes were also observed in the fifth lumbar vertebrae (LV) of KO mice (Fig. 3A-F). The reduction in the trabecular BV and changes in trabecular bone parameters were seen in both genders, and there was no gender–genotype interaction for any of the trabecular parameters (Fig. 3B-F). These data suggest that loss of Cldn-11 results in a dramatic reduction in trabecular BV at multiple skeletal sites in a gender-independent manner. In order to determine if loss of Cldn-11 influenced cortical bone, we evaluated cortical bone parameters at the mid-diaphyseal region of the femur and found no significant difference in TV, BV, or BV/TV between the KO and WT mice of either gender (Fig. 4A-D). Thus, a lack of Cldn-11 affects trabecular but not cortical bone.

Reduced bone formation in Cldn-11 KO mice

To determine the mechanism for a reduction in trabecular BV, we performed static histomorphometric analyses at the femoral secondary spongiosa taken from 12-week-old Cldn-11 KO and WT mice. Fig. 5A-D show that osteoid perimeter (O.Pm) and width (O.Wi) and osteoblast number (Ob.N) were significantly reduced in the Cldn-11 KO vs. WT mice. By contrast, neither TRAP-labeled osteoclast surface (Oc.S) nor osteoclast number (data not

shown) was significantly different between the two genotypes at this age (Fig. 5E). Consistent with the histomorphometric data, serum ALP activity but not TRAP activity was reduced in the Cldn-11 KO mice (Fig. 5F-G). Based on these data, we conclude that impaired bone formation and not increased bone resorption is the cause for reduced trabecular BV in Cldn-11 KO mice.

Cldn-11 modulates expression of osteoblast differentiation markers

Consistent with the histomorphometry and serum data, osteoblasts derived from Cldn-11 KO mice exhibited reduced expression of osteoblast differentiation markers *ALP*, *BSP*, and *DMP1* compared to osteoblasts derived from WT mice (Fig. 6A-C). As expected, *Cldn-11* expression was undetectable in Cldn-11 KO osteoblasts. However, expression levels of co-expressed *Cldn-12*, *Cldn-13*, and *Cldn-20* were unaffected (Fig. 6D). Furthermore, the ascorbic acid-induced increase in *ALP* mRNA expression is significantly reduced in Cldn-11 KO osteoblasts (data not shown). In RNA extracted from femoral and tibial trabecular bone from Cldn-11 KO mice, *BSP* was significantly reduced compared to wild-type bones, while there was no significant change in *Ctsk* expression (Fig. 6E).

In order to determine if Cldn-11 exerts direct effects on osteoblast differentiation, we overexpressed Cldn-11 by lentivirus (Lenti) transduction in pre-osteoblastic MC3T3-E1 cells which have very low basal Cldn-11 expression. As expected, Cldn-11 protein levels were increased by 48-fold in Lenti-Cldn-11 infected cells compared to Lenti-GFP transduced osteoblasts, comparable to the levels seen at day 8 of ascorbic acid-induced osteoblast differentiation. Cldn-11 overexpression stimulated expression of osteoblast differentiation markers as reflected by significant increases in *ALP* and *BSP* mRNA levels at day 6 (Fig. 7A,B). In contrast, Cldn-11 overexpression did not significantly change expression of osteoclast marker *RankL* (Fig. 7C). Furthermore, Alizarin Red staining revealed increased osteoblast differentiation in Cldn-11 overexpressing cells compared to GFP controls (Fig. 7D,E).

Tspan3 is expressed in osteoblasts and interacts with Cldn-11

To investigate the mechanism for Cldn-11 effects on osteoblast differentiation, we searched the literature for known interactions between Cldn-11 and other molecules. Tspan3 has been shown to interact with Cldn-11 in oligodendrocytes, where it was originally identified as a Cldn-11-associated protein in a yeast two-hybrid screen using Cldn-11 as bait.[32,33] In order to determine if Cldn-11–Tspan3 complexes exist in osteoblasts, total cellular lysate from Cldn-11 overexpressing MC3T3-E1 cells was immunoprecipitated with anti-Tspan3 and probed using anti-Cldn-11. Fig. 8A shows that Cldn-11 associates with Tspan3 in osteoblasts, and reverse immunoprecipitation with anti-Cldn-11 also pulled down Tspan3 (Fig. 8B). Immunostaining using Tspan3-specific antibody showed that, like Cldn-11, Tspan3 was expressed in osteoblast lining cells at the trabecular bone surface (Fig. 8C). *In vitro* studies showed that *Tspan3* expression also increased with osteoblast differentiation and exhibited a similar biphasic expression pattern to that of *Cldn-11* (Fig. 8D). Furthermore, we found that suppression of Tspan3 using lentiviral shRNA in MC3T3-E1 pre-osteoblasts inhibited osteoblast differentiation (Fig. 8E).

Cldn-11 modulates Notch signaling via ADAM10

Based on the finding that certain members of the Tspan family (Tspan5 and Tspan10) regulate cell functions via Notch signaling,[34] we investigated a model of Cldn-11 action that involves Cldn-11/Tspan3-mediated regulation of Notch signaling in osteoblasts. Consistent with this mode of action, we found that expression of Notch target signaling genes was significantly downregulated in Cldn-11 KO osteoblasts (Fig. 9A) but was upregulated in Cldn-11 overexpressing cultures (Fig. 9B). Furthermore, knockdown of Tspan3 using lentiviral shRNA reduced expression of Notch targets *Hey1* and *Hey2* in osteoblasts (Fig. 9C).

ADAM10 is a transmembrane protein that cleaves extracellular regions of several transmembrane target proteins, including Notch,[35] and we previously showed that osteoblasts express ADAM10.[36] Further, it was recently found that mutation of Tspan14 reduced ADAM10 surface expression and activity in human umbilical vein endothelial cells, [37] and a number of other Tspans, including Tspan5, Tspan10, Tspan15, Tspan17, and Tspan33, have been shown to regulate ADAM10 activity.[38-40] Notably, Tspan3 has also been found to regulate ADAM10 expression.[41] Therefore, we tested whether Cldn-11 overexpression modulated ADAM10 levels and found Cldn-11 overexpressing MC3T3-E1 cells express more mature ADAM10 than GFP control (Fig. 9D), Consistent with the involvement of Tspan3 in ADAM10 maturation, knockdown of Tspan3 reduced the amount of mature ADAM10 in MC3T3-E1 osteoblasts compared to control shRNA (Fig. 9E).

To determine if Cldn-11 regulates ADAM10-mediated activation of Notch signaling, GFP or Cldn-11 overexpressing MC3T3-E1 cells were treated with 10 μM GI254023 (an ADAM10-specific inhibitor)[42] or vehicle for 72 hours prior to immunoblotting for Notch intracellular domain (NICD)1. Fig. 9F shows that Cldn-11 overexpression increased NICD1 levels in cell lysates compared to GFP osteoblasts and that the Cldn-11 effect on increased NICD1 levels was blocked by pretreatment with the ADAM10 inhibitor. This effect on the NICD1 level is dependent on ADAM10. Furthermore, treatment with an ADAM10-specific inhibitor blocked the Cldn-11 effect on *ALP* mRNA levels in MC3T3-E1 cells (Fig. 9G). Interestingly, the ADAM10 inhibitor had no effect on *ALP* mRNA in GFP control cells. This lack of an effect may be due to the extremely low levels of basal Cldn-11 expression in MC3T3-E1 pre-osteoblasts, although further studies are needed to confirm this hypothesis.

Cldn-11 regulates articular cartilage

During the course of our IHC studies of Cldn-11 expression in bone, we found high levels of Cldn-11 expression in articular chondrocytes (Fig. 10A). Therefore, we evaluated the articular cartilage phenotype in 12-week-old Cldn-11 KO mice. Fig. 10B-E show reduced articular cartilage in Cldn-11 KO mice compared to control mice. Quantitation of articular cartilage revealed a 40% and 27% reduction in the articular cartilage area and thickness, respectively, in the Cldn-11 KO mice. To determine if Cldn-11 regulates chondrocyte differentiation, we overexpressed Cldn-11 in ATDC5 chondrocytes and found that Cldn-11 overexpression increased expression of articular cartilage markers and Notch targets compared to GFP overexpressing ATDC5 cells (Fig. 10F). Furthermore, immunostaining revealed decreased expression of Lubricin, a marker of immature articular chondrocytes

(Fig. 10G), and increased expression of Col10, a marker of differentiated chondrocytes (Fig. 10H), in articular cartilage of Cldn-11 KO mice.

Discussion

Cldn-11 was initially identified as oligodendrocyte-specific protein (OSP) that is primarily expressed in oligodendrocytes in the CNS, Sertoli cells in the testes, and the lateral wall of the cochlea.[8,9] Accordingly, targeted knockout (KO) of the *Cldn-11* gene results in CNS myelin defects, male sterility, and profound deafness in mice. Consistent with with our previously reported data,[22] the current study showed that expression of *Cldn-11* was increased by more than 50-fold during ascorbic acid (AA)-induced differentiation of normal mouse calvarial osteoblasts. Furthermore, immunohistochemistry (IHC) studies revealed high expression of Cldn-11 in osteoblast lining cells and in articular chondrocytes. Consistent with an important role for Cldn-11 in bone, we found that both trabecular bone mass and articular cartilage thickness were significantly reduced in the Cldn-11 KO mice compared to littermate controls in both genders. *In vitro* studies involving knockdown and overexpression of Cldn-11 revealed that Cldn-11 is a positive regulator of osteoblast differentiation. Interestingly, a recent study has found that Cldn-11 plays a positive role in osteoblastogenesis and a negative role in osteoclastogenesis via bidirectional EphB4–EphrinB2 signaling.[23] In addition, our studies on the mechanism of the Cldn-11 effect on osteoblasts reveal involvement of Tetraspanin (Tspan)3 and ADAM10 in mediating Cldn-11 actions on Notch signaling. Since our Cldn-11 KO mice lack global Cldn-11, however, future studies using mice with conditional disruption of Cldn-11 in osteoblasts and osteoclasts are needed to clarify the relative contributions of Cldn-11 from osteoblasts and osteoclasts to skeletal metabolism.

The large number of Cldn proteins, and the heterogeneity of their expression patterns, emphasizes their crucial role in the development and maintenance of various tissues. While the traditional role of Cldns is to control paracellular transport of small ions and other molecules, it is now becoming apparent that Cldns are intimately involved in signaling to and from tight junctions, providing cues for cell behaviors such as proliferation and differentiation.[6] The non-canonical action of Cldns seems to involve Cldn interactions with other proteins. In this regard, our previous work showed that Cldn-18 regulates osteoclast differentiation non-canonically by interacting with ZO-2 through its PDZ binding motif to modulate RANKL signaling.[19] The PDZ binding motif of Cldn-11 is different from that of Cldn-18, suggesting that these two Cldns may interact with other proteins via different mechanisms. Of note, unlike Tspan3, ZO-2 was not identified as a binding partner for Cldn-11 in a yeast two-hybrid screen.[32,33] In our studies of the mechanism through which Cldn-11 operates, we focused on Tspan3 based on our data that Tspan3 interacts with Cldn-11 in osteoblasts. Tspan proteins interact with one another, and with other integral membrane proteins, to form plasma membrane microdomains known as Tspan webs or Tspan enriched-microdomains (TEMs) that function to regulate many cellular processes by signal transduction through membrane receptors. Other Tspan proteins have been found to interact with Cldn family members.[43,44] Tspan5 and Tspan10 have been shown to be upregulated during osteoclast differentiation and involved in RANKL-induced fusion of osteoclast precursors,[34] but little is known about the role of any Tspan in osteoblasts or

chondrocytes. The findings of this study demonstrate for the first time that Tspan3 is highly expressed in osteoblasts, its expression increases during osteoblast differentiation, and it regulates osteoblast functions via modulation of Notch signaling.

Notch signaling has emerged as a critical regulator of mammalian skeletal tissues, where various genetic mouse models involving different molecular components of the Notch signaling pathway demonstrate that Notch critically controls postnatal bone homeostasis.[45] In osteoblasts, Notch signaling has been reported to either suppress or induce differentiation, depending on the context of cell type, differentiation status, time, and space. In terms of mechanisms for regulation of Notch signaling, cleavage of Notch by proteases has been proposed to play a key role.[45] The shedding of extracellular regions (ectodomains) of transmembrane proteins via proteolytic cleavage is emerging as an important mechanism for the regulation of cell development and function.[46]

ADAM10 is a transmembrane protease that cleaves extracellular regions of several transmembrane target proteins, including Notch.[35] Furthermore, other Tspans have been shown to regulate ADAM10 maturation and activity,[37-40] and Tspan3 itself has been shown to regulate ADAM10 expression.[41] Our studies show that the Cldn-11 effect on Notch signaling may be mediated via Tspan3 regulation of ADAM10 function. While our studies show that Cldn-11 and Tspan3 modulated levels of mature ADAM10, the mechanism for this regulation is yet to be established. The possible mechanisms by which Cldn-11/Tspan3 could regulate ADAM10 maturation and activity include stabilization of ADAM10 at the plasma membrane, increase in ADAM10 expression, and modulation of the exit of ADAM10 from the endoplasmic reticulum.

An important role for Notch signaling in the development and maintenance of articular cartilage, and in development of osteoarthritis, has been well established.[47] Based on our data that Cldn-11 is highly expressed in articular chondrocytes and that Cldn-11 KO mice exhibited significant reduction in articular cartilage thickness and area, we evaluated whether Cldn-11 regulated expression of articular cartilage markers. Our findings show that Cldn-11 overexpression increased expression of markers of articular chondrocytes. However, additional studies are needed to determine if the Cldn-11 effect on articular chondrocytes is mediated via Tspan3 interaction and ADAM10-mediated regulation of Notch signaling.

ADAM10 maturation and membrane localization are regulated by direct protein–protein interactions.[48] Based on the findings that Tspans interact with ADAM10, and that osteoregulatory agents such as BMPs, IGF-I, vitamin D, and the Wnts interact with ADAM10 expression and activity[49-52] and modulate expression of Tspan3 interacting protein Cldn-11, it is possible that bone formation regulators may mediate the formation of the Cldn-11/Tspan3/ADAM10 complex to modulate ADAM10-mediated regulation of growth factor signaling pathways. Since a deficiency in growth factor signaling pathways[53] has been shown to be a major contributing factor to impaired bone formation during aging and glucocorticoid treatment, our future studies will investigate whether the Cldn-11/Tspan3/ADAM10 complex is altered in osteoblasts during disease states.

While this study presents Cldn-11, Tspan3, and ADAM10 as a novel complex of proteins which potentially represent new druggable targets for osteoporosis, further studies are needed to clarify the mechanisms involved. In particular, since Cldn-11 is highly expressed in nervous tissue, it is possible that a neural phenotype contributes to the skeletal changes observed in Cldn-11 KO mice, although we observed no evidence of changes in grip strength or a disuse phenotype. Additionally, while we have demonstrated the involvement of Notch signaling in this Cldn-11/Tspan3/ADAM10 pathway, it is known that Notch is regulated by many factors, and many other signaling pathways are regulated by Cldns. As such, it is important for the role of Notch signaling in mediating Cldn-11 effects on osteoblasts, as well as the extent to which these effects are mediated via ADAM10, to be confirmed in an unbiased pathway analysis in the future. However, this novel pathway opens new possibilities for developing sorely needed therapies for the prevention and treatment of osteoporosis and other debilitating bone diseases.

Supplementary Material

Refer to Web version on PubMed Central for supplementary material.

Acknowledgments

The authors would like to thank Ms. Nancy Lowen, Ms. Heather Watt, and Dr. Shaohong Cheng for their expert technical assistance. Cherie Southwood of the Center for Molecular Medicine and Genetics at Wayne State University generated the embryo image in Fig. 1. All other work was performed with the facilities provided by the US Department of Veterans Affairs in Loma Linda, CA. This work was supported by National Institutes of Health grants R01 AR070806 to SM, 2 R25 GM060507 to Loma Linda University Center for Health Disparities and Molecular Medicine/Initiative for Maximizing Student Development, and R01 DC006262 to AG.

RCL, WX, and SM designed experiments and performed data analysis and interpretation. RCL, WX, CG, and SP performed experiments. SM, RCL, WX, and AG wrote the manuscript. SM conceived and oversaw the entire the project.

Grant support: National Institutes of Health grants R01 AR070806 (to SM), 2 R25 GM060507 (to LLU CHDMM/IMSD), and R01 DC006262 (to AG). The authors have nothing to disclose.

References

1. Drake MT, Khosla S. Sex Steroids and the Pathogenesis of Osteoporosis In: Bilezikian JP, editor. Primer on the Metabolic Bone Diseases and Disorders of Mineral Metabolism. 9th ed. John Wiley & Sons, Inc 2019 pp. 412–8.
2. Angelow S, Ahlstrom R, Yu AS. Biology of claudins. Am J Physiol Renal Physiol. 2008 10;295(4):F867–76. [PubMed: 18480174]
3. Elkouby-Naor L, Ben-Yosef T. Functions of claudin tight junction proteins and their complex interactions in various physiological systems. Int Rev Cell Mol Biol. 2010;279:1–32. [PubMed: 20797675]
4. Krause G, Winkler L, Mueller SL, Haseloff RF, Piontek J, Blasig IE. Structure and function of claudins. Biochim. Biophys. Acta. 2008 3;1778(3):631–45. [PubMed: 18036336]
5. Mineta K, Yamamoto Y, Yamazaki Y, Tanaka H, Tada Y, Saito K, Tamura A, Igarashi M, Endo T, Takeuchi K, Tsukita S. Predicted expansion of the claudin multigene family. FEBS Lett. 2011 2;585(4):606–12. [PubMed: 21276448]
6. Alshbool FZ, Mohan S. Emerging multifunctional roles of Claudin tight junction proteins in bone. Endocrinology. 2014 7;155(7):2363–76. [PubMed: 24758302]
7. Hagen SJ. Non-canonical functions of claudin proteins: Beyond the regulation of cell-cell adhesions. Tissue Barriers. 2017 3;5(2):e1327839. [PubMed: 28548895]

8. Gow A, Southwood CM, Li JS, Pariali M, Riordan GP, Brodie SE, Danias J, Bronstein JM, Kachar B, Lazzarini RA. CNS myelin and sertoli cell tight junction strands are absent in Osp/claudin-11 null mice. Cell. 1999 12;99(6):649–59. [PubMed: 10612400]

9. Gow A, Davies C, Southwood CM, Frolenkov G, Chrustowski M, Ng L, Yamauchi D, Marcus DC, Kachar B. Deafness in Claudin 11-null mice reveals the critical contribution of basal cell tight junctions to stria vascularis function. J Neurosci. 2004 8;24(32):7051–62. [PubMed: 15306639]

10. Devaux J, Gow A. Tight junctions potentiate the insulative properties of small CNS myelinated axons. J. Cell Biol. 2008 12;183(5):909–21. [PubMed: 19047465]

11. Maheras KJ, Peppi M, Ghoddoussi F, Galloway MP, Perrine SA, Gow A. Absence of Claudin 11 in CNS Myelin Perturbs Behavior and Neurotransmitter Levels in Mice. Sci Rep. 2018 2;8(1):3798. [PubMed: 29491447]

12. Ben-Yosef T, Belyantseva IA, Saunders TL, Hughes ED, Kawamoto K, Van Itallie CM, Beyer LA, Halsey K, Gardner DJ, Wilcox ER, Rasmussen J, Anderson JM, Dolan DF, Forge A, Raphael Y, Camper SA, Friedman TB. Claudin 14 knockout mice, a model for autosomal recessive deafness DFNB29, are deaf due to cochlear hair cell degeneration. Hum Mol Genet. 2003 8;12(16):2049–61. [PubMed: 12913076]

13. Furuse M, Hata M, Furuse K, Yoshida Y, Haratake A, Sugitani Y, Noda T, Kubo A, Tsukita S. Claudin-based tight junctions are crucial for the mammalian epidermal barrier: A lesson from claudin-1-deficient mice. J Cell Biol. 2002 3;156(6):1099–111. [PubMed: 11889141]

14. Nitta T, Hata M, Gotoh S, Seo Y, Sasaki H, Hashimoto N, Furuse M, Tsukita S. Size-selective loosening of the blood-brain barrier in claudin-5-deficient mice. J Cell Biol. 2003 5;161(3):653–60. [PubMed: 12743111]

15. Tatum R, Zhang Y, Salleng K, Lu Z, Lin JJ, Lu Q, Jeansonne BG, Ding L, Chen YH. Renal salt wasting and chronic dehydration in claudin-7-deficient mice. Am J Physiol Renal Physiol. 2010 1;298(1):F24–34. [PubMed: 19759267]

16. Will C, Breiderhoff T, Thumfart J, Stuiver M, Kopplin K, Sommer K, Gunzel D, Querfeld U, Meij IC, Shan Q, Bleich M, Willnow TE, Muller D. Targeted deletion of murine Cldn16 identifies extra- and intrarenal compensatory mechanisms of Ca2+ and Mg2+ wasting. Am J Physiol Renal Physiol. 2010 5;298(5):F1152–61. [PubMed: 20147368]

17. Hou J, Renigunta A, Gomes AS, Hou M, Paul DL, Waldegger S, Goodenough DA. Claudin-16 and claudin-19 interaction is required for their assembly into tight junctions and for renal reabsorption of magnesium. Proc Natl Acad Sci U S A. 2009 9;106(36):15350–5. [PubMed: 19706394]

18. Tamura A, Kitano Y, Hata M, Katsuno T, Moriwaki K, Sasaki H, Hayashi H, Suzuki Y, Noda T, Furuse M, Tsukita S, Tsukita S. Megaintestine in claudin-15-deficient mice. Gastroenterology. 2008 2;134(2):523–34. [PubMed: 18242218]

19. Linares GR, Brommage R, Powell DR, Xing W, Chen ST, Alshbool FZ, Lau KH, Wergedal JE, Mohan S. Claudin 18 is a novel negative regulator of bone resorption and osteoclast differentiation. J Bone Miner Res. 2012 7;27(7):1553–65. [PubMed: 22437732]

20. Kim HY, Alarcon C, Pourteymour S, Wergedal JE, Mohan S. Disruption of claudin-18 diminishes ovariectomy-induced bone loss in mice. Am J Physiol Endocrinol Metab. 2013 3;304(5):E531–7. [PubMed: 23299504]

21. Alshbool FZ, Alarcon C, Wergedal J, Mohan S. A high-calcium diet failed to rescue an osteopenia phenotype in claudin-18 knockout mice. Physiol Rep. 2014 1;2(1):e00200. [PubMed: 24744879]

22. Alshbool FZ, Mohan S. Differential expression of claudin family members during osteoblast and osteoclast differentiation: Cldn-1 is a novel positive regulator of osteoblastogenesis. PLoS ONE. 2014;9(12):e114357. [PubMed: 25479235]

23. Baek JM, Cheon Y-H, Kwak SC, Jun HY, Yoon K-H, Lee MS, Kim J-Y. Claudin 11 regulates bone homeostasis via bidirectional EphB4-EphrinB2 signaling. Exp. Mol. Med. 2018 4;50(4):50. [PubMed: 29700355]

24. Miyakoshi N, Richman C, Kasukawa Y, Linkhart TA, Baylink DJ, Mohan S. Evidence that IGF-binding protein-5 functions as a growth factor. J Clin Invest. 2001 1;107(1):73–81. [PubMed: 11134182]

25. Bradley EW, Oursler MJ. Osteoclast culture and resorption assays. Methods Mol Biol. 2008;455:19–35. [PubMed: 18463808]

26. Cheng S, Xing W, Pourteymoor S, Mohan S. Conditional disruption of the prolyl hydroxylase domain-containing protein 2 (Phd2) gene defines its key role in skeletal development. J Bone Miner Res. 2014 10;29(10):2276–86. [PubMed: 24753072]
27. Bouxsein ML, Boyd SK, Christiansen BA, Guldberg RE, Jepsen KJ, Müller R. Guidelines for assessment of bone microstructure in rodents using micro-computed tomography. J. Bone Miner. Res. 2010 7;25(7):1468–86. [PubMed: 20533309]
28. Xing W, Kim J, Wergedal J, Chen S-T, Mohan S. Ephrin B1 regulates bone marrow stromal cell differentiation and bone formation by influencing TAZ transactivation via complex formation with NHERF1. Mol. Cell. Biol. 2010 2;30(3):711–21. [PubMed: 19995908]
29. Iida A, Xing W, Docx MKF, Nakashima T, Wang Z, Kimizuka M, Van Hul W, Rating D, Spranger J, Ohashi H, Miyake N, Matsumoto N, Mohan S, Nishimura G, Mortier G, Ikegawa S. Identification of biallelic LRRK1 mutations in osteosclerotic metaphyseal dysplasia and evidence for locus heterogeneity. J. Med. Genet. 2016 8;53(8):568–74. [PubMed: 27055475]
30. Linares GR, Xing W, Govoni KE, Chen ST, Mohan S. Glutaredoxin 5 regulates osteoblast apoptosis by protecting against oxidative stress. Bone. 2009 5;44(5):795–804. [PubMed: 19442627]
31. Cheng S, Zhao SL, Nelson B, Kesavan C, Qin X, Wergedal J, Mohan S, Xing W. Targeted disruption of ephrin B1 in cells of myeloid lineage increases osteoclast differentiation and bone resorption in mice. PLoS ONE. 2012;7(3):e32887. [PubMed: 22403721]
32. Tiwari-Woodruff SK, Buznikov AG, Vu TQ, Micevych PE, Chen K, Kornblum HI, Bronstein JM. OSP/claudin-11 forms a complex with a novel member of the tetraspanin super family and beta1 integrin and regulates proliferation and migration of oligodendrocytes. J Cell Biol. 2001 4;153(2): 295–305. [PubMed: 11309411]
33. Tiwari-Woodruff SK, Kaplan R, Kornblum HI, Bronstein JM. Developmental expression of OAP-1/Tspan-3, a member of the tetraspanin superfamily. J. Neurosci. Res. 2004 7;77(2):166–73. [PubMed: 15211584]
34. Zhou J, Fujiwara T, Ye S, Li X, Zhao H. Downregulation of Notch modulators, tetraspanin 5 and 10, inhibits osteoclastogenesis in vitro. Calcif. Tissue Int. 2014 9;95(3):209–17. [PubMed: 24935633]
35. Weber S, Saftig P. Ectodomain shedding and ADAMs in development. Development. 2012 10;139(20):3693–709. [PubMed: 22991436]
36. Mohan S, Thompson GR, Amaar YG, Hathaway G, Tschesche H, Baylink DJ. ADAM-9 is an insulin-like growth factor binding protein-5 protease produced and secreted by human osteoblasts. Biochemistry. 2002 12;41(51):15394–403. [PubMed: 12484779]
37. Noy PJ, Yang J, Reyat JS, Matthews AL, Charlton AE, Furmston J, Rogers DA, Rainger GE, Tomlinson MG. TspanC8 Tetraspanins and A Disintegrin and Metalloprotease 10 (ADAM10) Interact via Their Extracellular Regions: EVIDENCE FOR DISTINCT BINDING MECHANISMS FOR DIFFERENT TspanC8 PROTEINS. J. Biol. Chem. 2016 2;291(7):3145–57. [PubMed: 26668317]
38. Matthews AL, Koo CZ, Szyroka J, Harrison N, Kanhere A, Tomlinson MG. Regulation of Leukocytes by TspanC8 Tetraspanins and the “Molecular Scissor” ADAM10. Front Immunol. 2018;9:1451. [PubMed: 30013551]
39. Yeung L, Hickey MJ, Wright MD. The Many and Varied Roles of Tetraspanins in Immune Cell Recruitment and Migration. Front Immunol. 2018;9:1644. [PubMed: 30072994]
40. Shah J, Rouaud F, Guerrera D, Vasileva E, Popov LM, Kelley WL, Rubinstein E, Carette JE, Amieva MR, Citi S. A Dock-and-Lock Mechanism Clusters ADAM10 at Cell-Cell Junctions to Promote α-Toxin Cytotoxicity. Cell Rep. 2018 11;25(8):2132–2147.e7. [PubMed: 30463011]
41. Seipold L, Damme M, Prox J, Rabe B, Kasparek P, Sedlacek R, Altmeppen H, Willem M, Boland B, Glatzel M, Saftig P. Tetraspanin 3: A central endocytic membrane component regulating the expression of ADAM10, presenilin and the amyloid precursor protein. Biochim Biophys Acta Mol Cell Res. 2017 1;1864(1):217–30. [PubMed: 27818272]
42. Schlomann U, Dorzweiler K, Nuti E, Tuccinardi T, Rossello A, Bartsch JW. Metalloprotease inhibitor profiles of human ADAM8 in vitro and in cell-based assays. Biol. Chem. 2019 3;

43. Sun S, Jin G, Kang H. CD81 and CLDN1 polymorphisms and hepatitis C virus infection susceptibility: A case control study. Gene. 2015 8;567(1):87–91. [PubMed: 25934191]
44. Kovalenko OV, Yang XH, Hemler ME. A novel cysteine cross-linking method reveals a direct association between claudin-1 and tetraspanin CD9. Mol. Cell Proteomics. 2007 11;6(11):1855–67. [PubMed: 17644758]
45. Canalis E Notch in skeletal physiology and disease. Osteoporos Int. 2018 12;29(12):2611–21. [PubMed: 30194467]
46. Lichtenthaler SF, Lemberg MK, Fluhrer R. Proteolytic ectodomain shedding of membrane proteins in mammals-hardware, concepts, and recent developments. EMBO J. 2018 8;37(15).
47. Saito T, Tanaka S. Molecular mechanisms underlying osteoarthritis development: Notch and NF-κB. Arthritis Res. Ther. 2017 5;19(1):94. [PubMed: 28506315]
48. Endres K, Fahrenholz F. Regulation of α-secretase ADAM10 expression and activity. Exp Brain Res. 2012 4;217(3–4):343–52. [PubMed: 21969210]
49. Wan X-Z, Li B, Li Y-C, Yang X-L, Zhang W, Zhong L, Tang S-J. Activation of NMDA receptors upregulates a disintegrin and metalloproteinase 10 via a Wnt/MAPK signaling pathway. J. Neurosci. 2012 3;32(11):3910–6. [PubMed: 22423111]
50. Wang L, Liu Z, Shi H, Liu J. Two Paralogous Tetraspanins TSP-12 and TSP-14 Function with the ADAM10 Metalloprotease SUP-17 to Promote BMP Signaling in Caenorhabditis elegans. PLoS Genet. 2017 1;13(1):e1006568. [PubMed: 28068334]
51. Yang WS, Kim JJ, Han NJ, Lee EK, Park S-K. 1,25-Dihydroxyvitamin D3 Attenuates the Effects of Lipopolysaccharide by Causing ADAM10-Dependent Ectodomain Shedding of Toll-Like Receptor 4. Cell. Physiol. Biochem. 2017;41(5):2104–16. [PubMed: 28427048]
52. Park GB, Kim D. Insulin-like growth factor-1 activates different catalytic subunits p110 of PI3K in a cell-type-dependent manner to induce lipogenesis-dependent epithelial-mesenchymal transition through the regulation of ADAM10 and ADAM17. Mol. Cell. Biochem. 2018 2;439(1–2):199–211. [PubMed: 28819788]
53. Lindsey RC, Mohan S. Skeletal effects of growth hormone and insulin-like growth factor-I therapy. Mol. Cell. Endocrinol. 2016 5;432:44–55. [PubMed: 26408965]

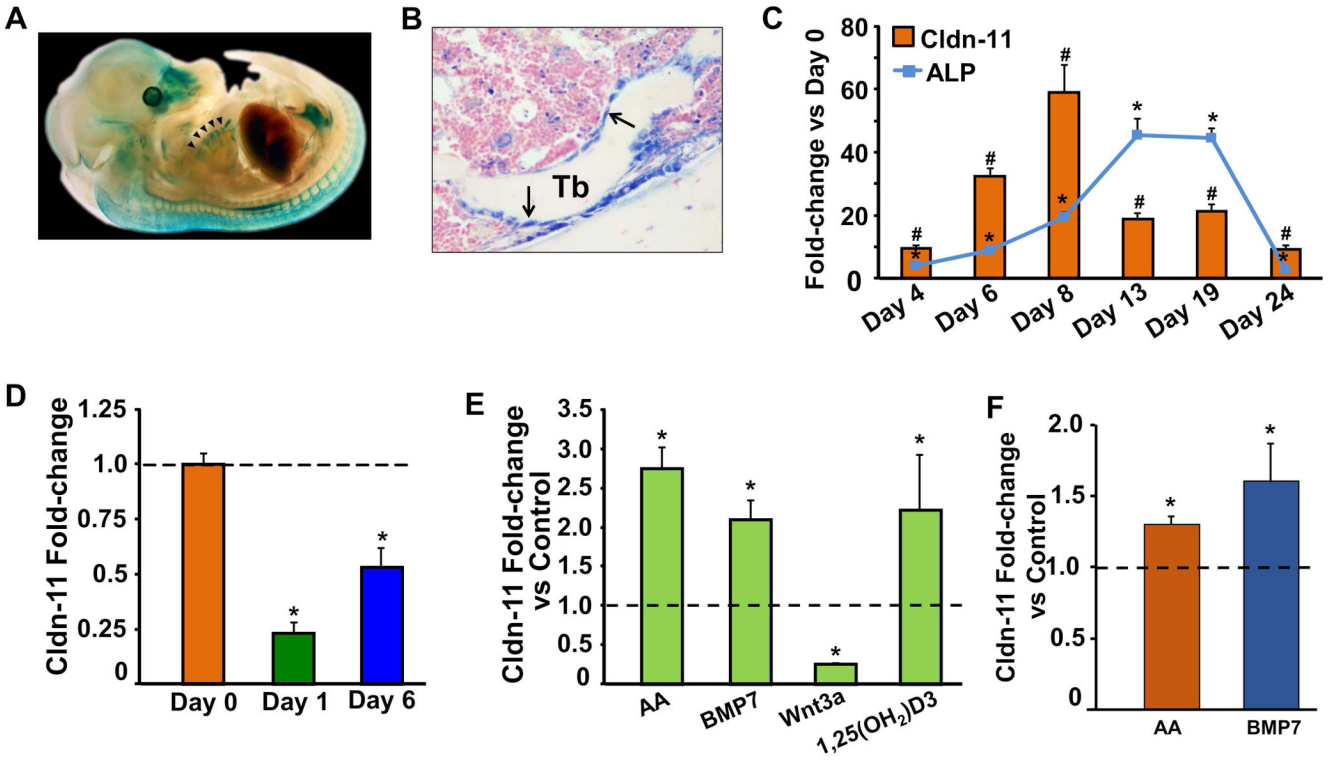

Fig. 1.

Cldn-11 is expressed in bone cells. (A) Mouse embryo at embryonic day 14.5 stained for β-galactosidase activity demonstrates Cldn-11 expression, particularly in long bones such as the ribs (black arrowheads). (B) Immunohistochemical detection of Cldn-11 in the lining cells of secondary spongiosa of 12-week-old mice. Tb, trabecular bone. Blue stain indicates Cldn-11 expression. Arrows show lining cells. (C) Expression levels of *Cldn-11* and *ALP* during AA-induced differentiation of calvarial osteoblasts derived from 3-day-old mice. Values are fold-change vs. day 0 (mean ± SEM, n = 6). $^{\#}P < 0.05$ vs. *Cldn-11* day 0, $^{*}P < 0.05$ vs. *ALP* day 0. (D) Expression levels of *Cldn-11* during MCSF- and RANKL-induced differentiation of mouse bone marrow macrophages into osteoclasts. Values are fold-change vs. day 0 (mean ± SEM, n = 6). $^{*}P < 0.05$ vs. day 0. (E) Effects of 24-hour treatment with AA (50 μg/mL), BMP7 (10 ng/mL), Wnt3a (10 ng/mL) and $1,25(OH)_2D_3$ (10 nM) on *Cldn-11* mRNA levels in cultures of normal mouse calvarial osteoblasts derived from 3-day-old mice. Values are fold-change vs. vehicle control (mean ± SEM, n = 6). $^{*}P < 0.05$ vs. vehicle. (F) Effects of 24-hour treatment with AA (50 μg/mL) and BMP7 (10 ng/mL) on *Cldn-11* mRNA levels in normal human osteoblasts derived from rib. Values are fold-change vs. vehicle control (mean ± SEM, n = 4). $^{*}P < 0.05$ vs. vehicle.

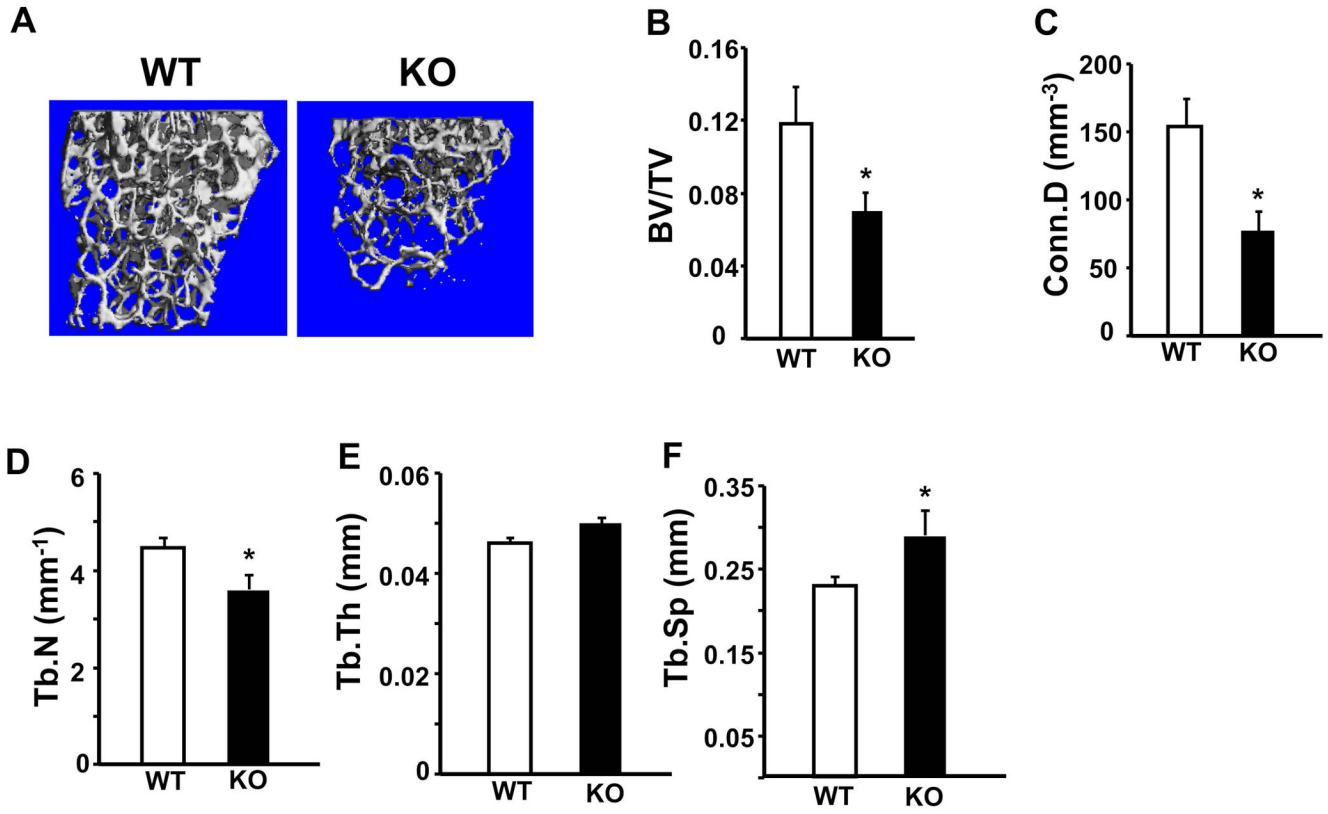

Fig. 2.

Trabecular bone is decreased in the distal femur of Cldn-11 KO mice at 12 weeks of age. (A) Representative microCT images of the secondary spongiosa region of distal femur from female mice. (B) Bone volume (BV)/tissue volume (TV). (C) Connectivity density (Conn.D). (D) Trabecular number (Tb.N). (E) Trabecular thickness (Tb.Th). (F) Trabecular separation (Tb.Sp). Values are mean ± SEM of 12-week old wild type (WT) control and KO mice. *$P < 0.05$ vs. control mice (n = 10–12 per group).

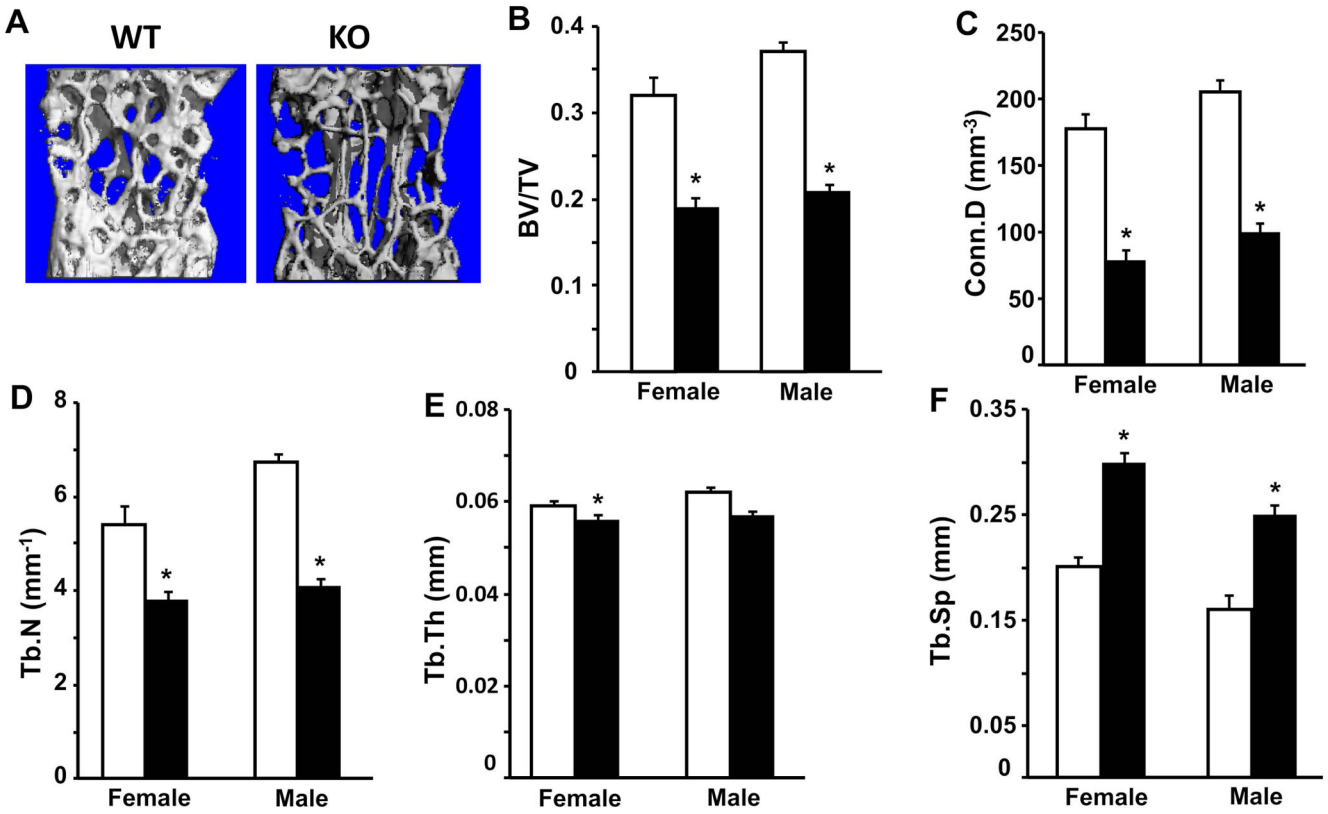

Fig. 3.

Trabecular bone is decreased in the fifth lumbar vertebrae (LV5) of male and female Cldn-11 KO mice at 12 weeks of age. (A) Representative microCT images of the secondary spongiosa region of LV5. (B) Bone volume (BV)/tissue volume (TV). (C) Connectivity density (Conn.D). (D) Trabecular number (Tb.N). (E) Trabecular thickness (Tb.Th). (F) Trabecular separation (Tb.Sp). Values are mean ± SEM of 12-week-old wild type (WT) control (white bars) and KO (black bars) mice. $*P < 0.05$ vs. control mice (n = 5–6 per group).

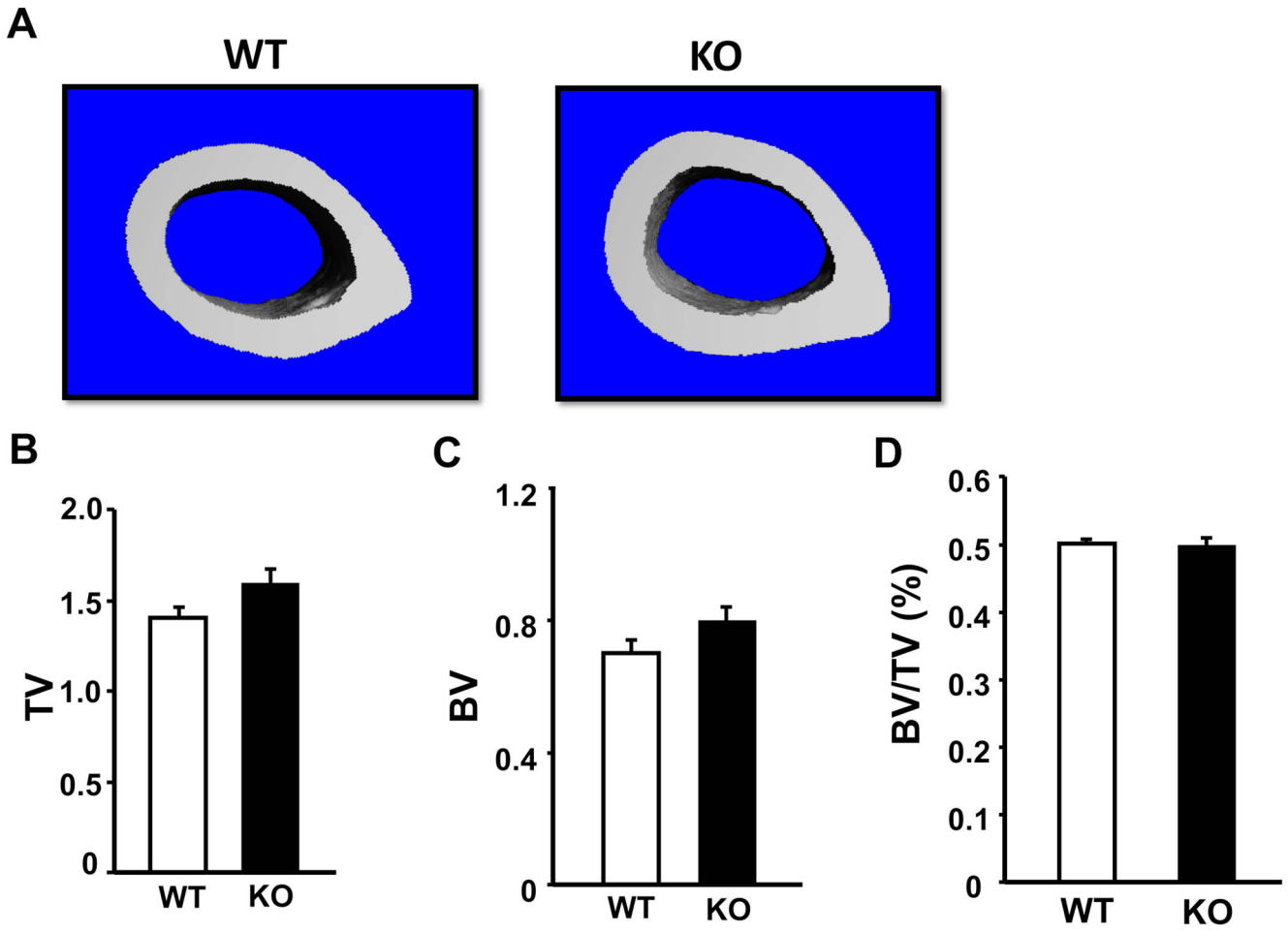

Fig. 4.

Cortical bone is unchanged at the mid-diaphysis of Cldn-11 KO female mice at 12 weeks of age. (A) Representative microCT images of the mid-diaphysis of female WT and KO mice. (B) Tissue volume (TV). (C) Bone volume (BV). (D) Bone volume/tissue volume (BV/TV). Values are mean ± SEM of 12-week-old wild type (WT) control and KO mice (n = 5–6 per group).

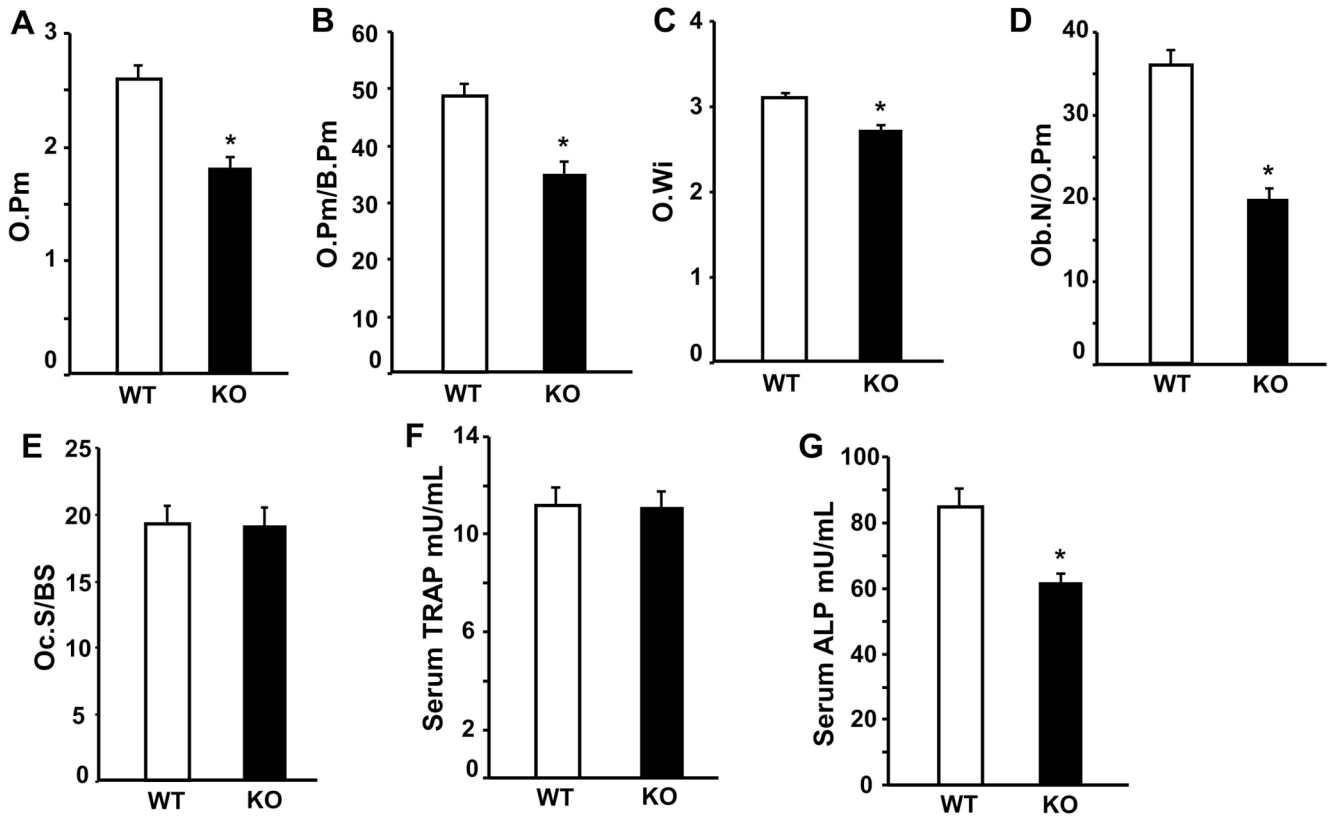

Fig. 5.

Bone formation but not resorption parameters are decreased in Cldn-11 KO mice at 12 weeks of age. (A) Osteoid perimeter (O.Pm). (B) Osteoid perimeter (O.Pm) adjusted for bone perimeter (B.Pm). (C) Osteoid width (O.Wi). (D) Osteoblast number (Ob.N) adjusted for osteoid perimeter (O.pm). (E) Osteoclast surface (Oc.S) adjusted for bone surface (BS). (F) Activity levels of serum tartrate-resistant acid phosphatase (TRAP). (G) Activity levels of serum alkaline phosphatase (ALP). Values are mean ± SEM of 12-week-old wild type (WT) control and KO mice. *$P < 0.05$ vs. control mice (n = 10–12 per group).

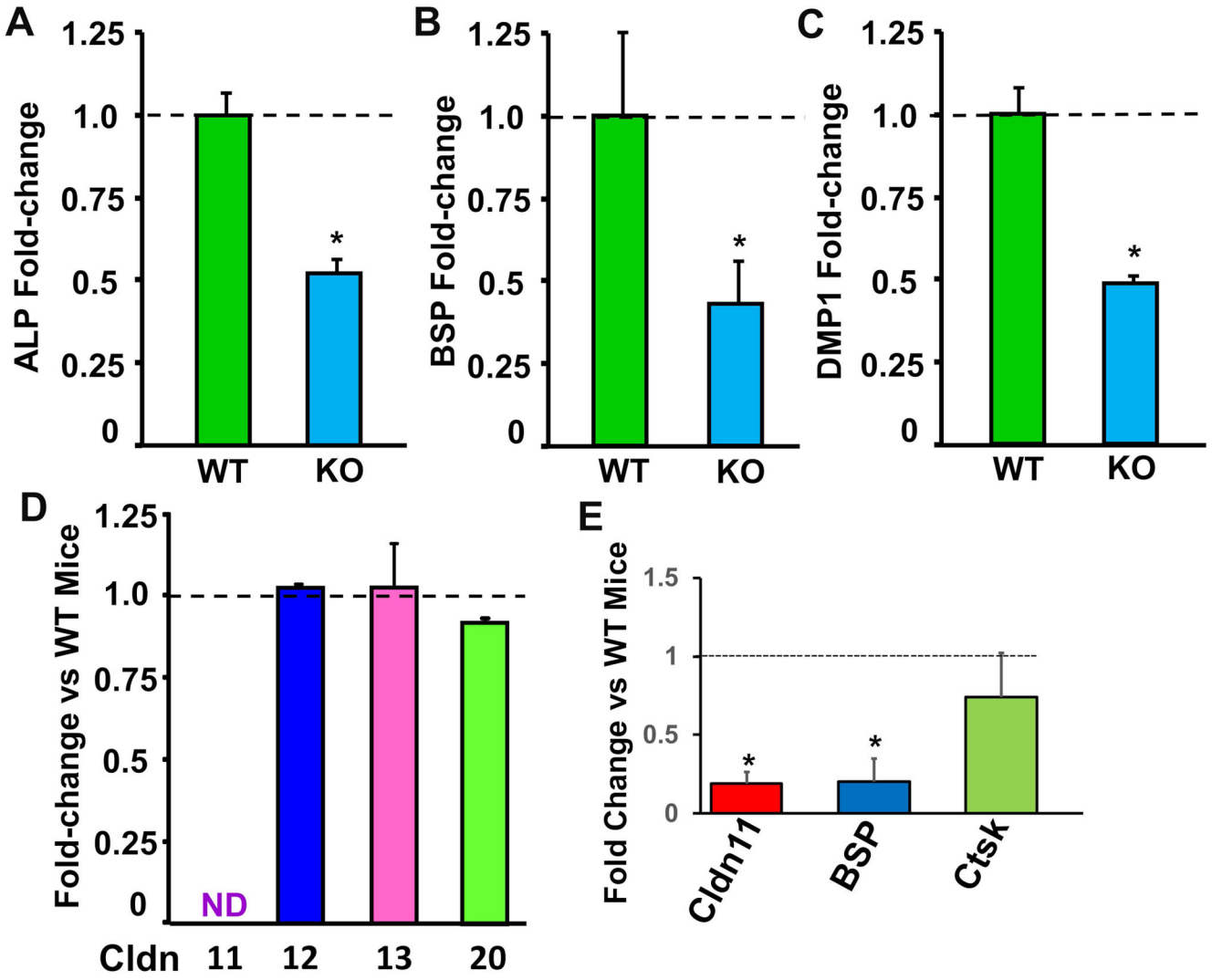

Fig. 6.

Osteoblast differentiation marker genes are decreased in Cldn-11 KO mice. Calvarial osteoblasts derived from wild-type (WT) and Cldn-11 knockout (KO) mice were grown in serum-free culture for six days prior to RNA extraction. (A) *ALP* mRNA levels in osteoblasts derived from WT and KO mice. (B) *BSP* mRNA levels in osteoblasts derived from WT and KO mice. (C) *DMP1* mRNA levels in osteoblasts derived from WT and KO mice. (D) *Cldn-11*, *Cldn-12*, *Cldn-13*, and *Cldn-20* mRNA levels in osteoblasts derived from WT and KO mice. (E) *Cldn-11*, *BSP*, and *Ctsk* mRNA levels in femoral and tibial trabecular bone from WT and KO mice. Values (mean ± SEM; n = 4 for osteoblast studies, n = 7 for bone tissue studies) are fold-change vs. WT. **P* < 0.05 vs. WT.

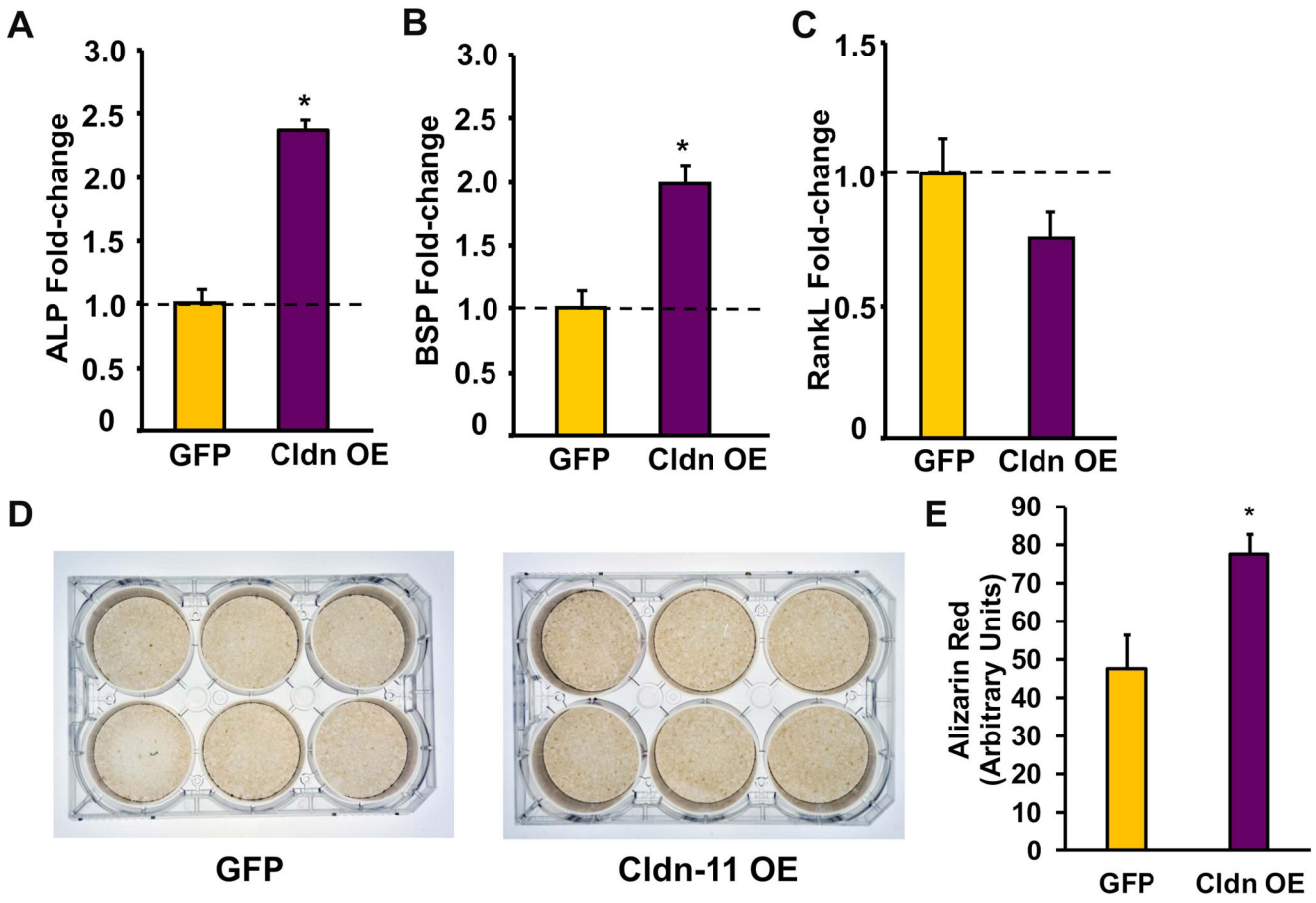

Fig. 7.

Osteoblast differentiation marker genes and Alizarin Red staining are increased in Cldn-11 overexpressing cells. Lentiviral vectors were used to overexpress Cldn-11 or GFP control in MC3T3-E1 cells which were grown in serum-free culture for six days prior to RNA extraction. (A) *ALP* mRNA levels in GFP overexpressing (control) and Cldn-11 overexpressing cells. (B) *BSP* mRNA levels in GFP and Cldn-11 overexpressing cells. (C) *RankL* mRNA levels in GFP and Cldn-11 overexpressing cells. (D) GFP and Cldn-11 overexpressing cells were grown in culture for 23 days before Alizarin Red staining. (E) Quantitated Alizarin Red staining from GFP and Cldn-11 overexpressing cells. Values (mean ± SEM; n = 4 for RNA studies, n = 6 for staining studies) are fold-change vs. GFP overexpressing osteoblasts. $*P < 0.05$ vs. GFP control osteoblasts.

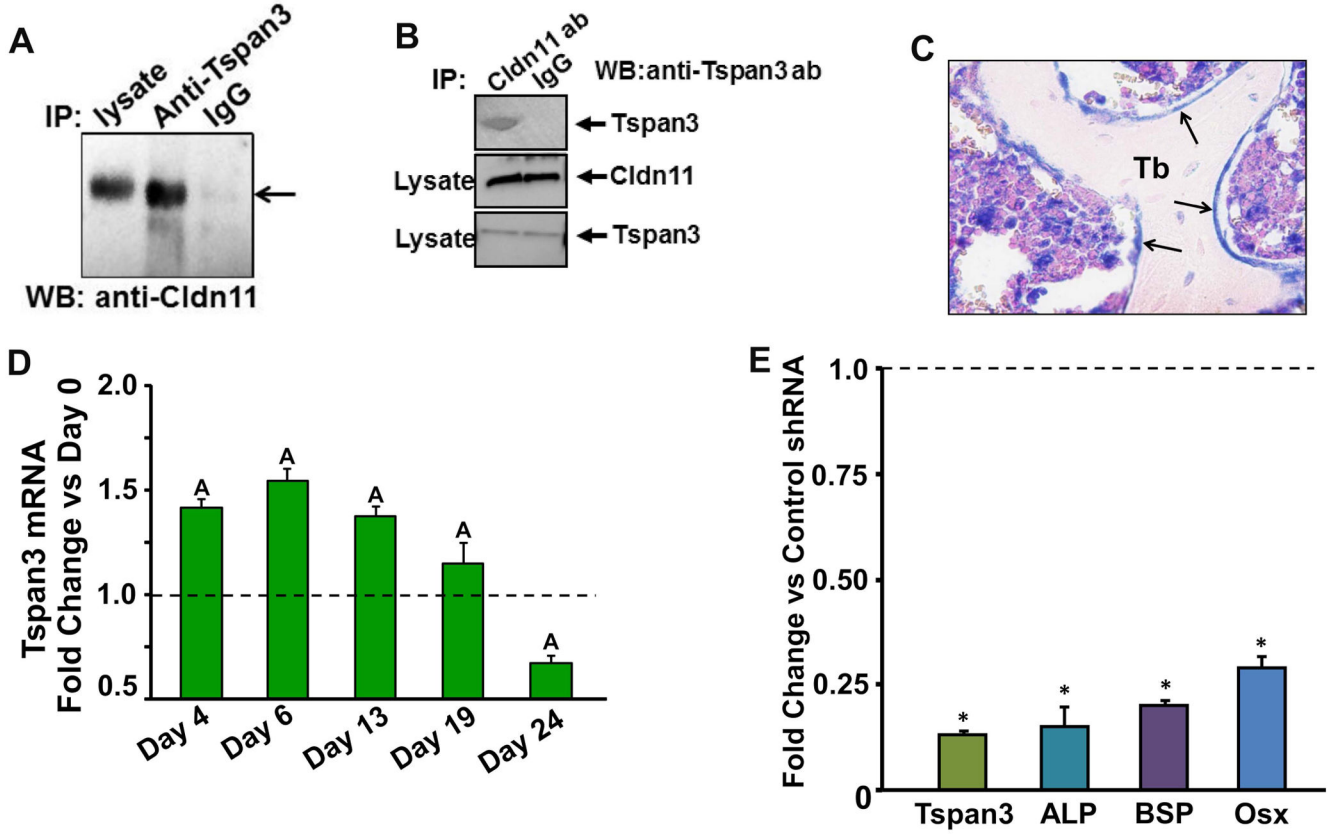

Fig. 8.

Tetraspanin (Tspan)3 is expressed in osteoblasts and interacts with Cldn-11. (A) Tspan3 interacts with Cldn-11 in osteoblasts. Total cellular lysates from Cldn-11 overexpressing MC3T3-E1 osteoblasts were immunoprecipitated with anti-Tspan3 or control IgG and probed using anti-Cldn-11. Arrow shows location of Cldn-11. (B) Total cellular lysates from Cldn-11 overexpressing MC3T3-E1 osteoblasts were immunoprecipitated with anti-Cldn-11 and probed using anti-Tspan3. (C) Immunohistochemical detection of Tspan3 in the lining cells of the secondary spongiosa of a 12-week-old WT mouse. Tb, trabecular bone. Arrows show lining cells. (D) *Tspan3* mRNA levels during AA-induced differentiation of osteoblasts derived from calvariae of 3-day-old mice. Values are fold-change vs. day 0 (mean ± SEM, n = 6). $*P < 0.05$ vs. day 0. (E) Tspan3 knockdown in MC3T3-E1 cells impairs osteoblast differentiation. *Tspan3*, *ALP*, *BSP*, and *Osx* mRNA levels in lentiviral Tspan3 shRNA and control shRNA infected cultures. Values (mean ± SEM, n = 4) are fold-change vs. control shRNA cultures. $*P < 0.05$ vs. control shRNA.

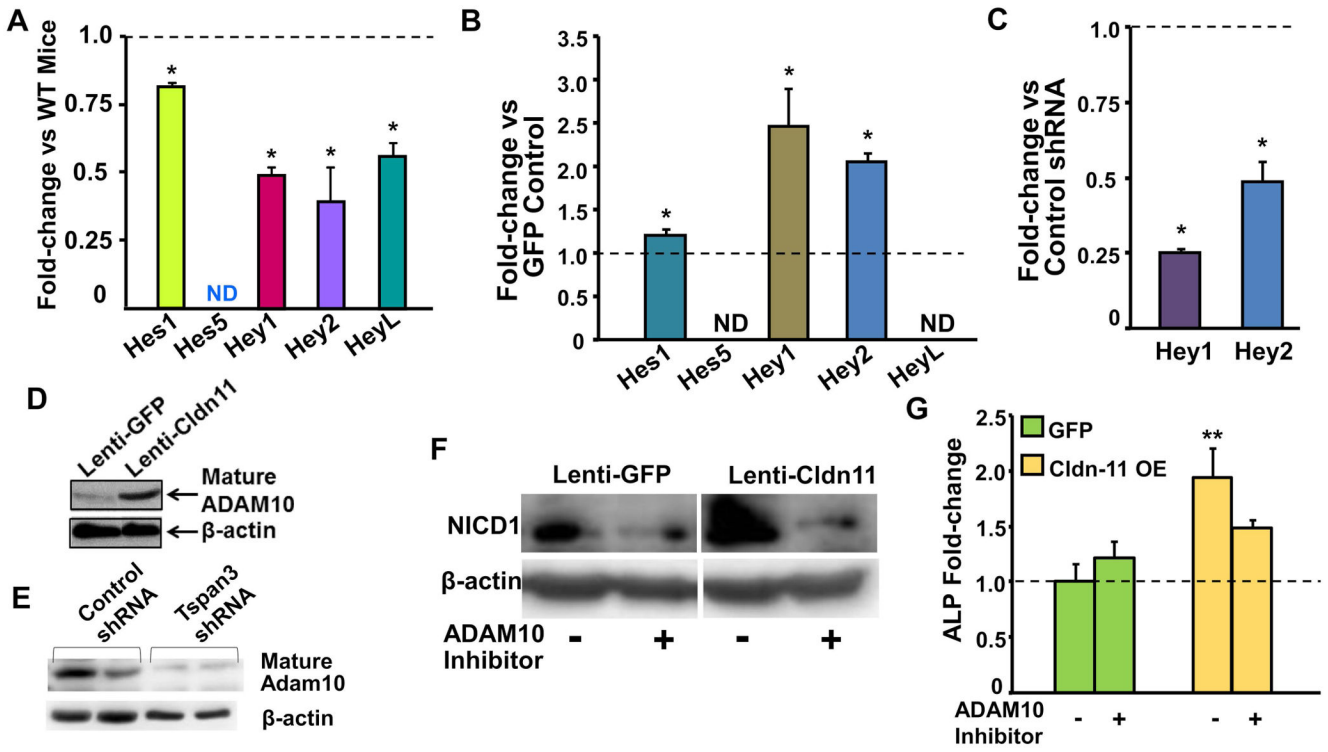

Fig. 9.

Cldn-11 modulates ADAM10 and Notch targets in osteoblasts. (A) Notch target gene mRNA levels in osteoblasts derived from WT and KO mice. Values (mean ± SEM, n = 4) are fold-change of WT mice. *$P < 0.05$ vs. WT mice. (B) Notch target gene mRNA levels in GFP overexpressing control and Cldn-11 overexpressing MC3T3-E1 osteoblasts. Values (mean ± SEM, n = 4) are fold-change vs. GFP control. *$P < 0.05$ vs. GFP control. ND, not detectable. (C) Notch target gene *Hey1* and *Hey2* mRNA levels in MC3T3-E1 osteoblasts expressing control shRNA and Tspan3 shRNA. Values (mean ± SEM, n = 4) are fold-change of control shRNA. *$P < 0.05$ vs. control shRNA. (D) Immunoblot analysis of mature ADAM10 levels in cell lysates of GFP or Cldn-11 overexpressing MC3T3-E1 osteoblasts. (E) Immunoblot analysis of mature ADAM10 levels in MC3T3-E1 cells expressing control or Tspan3 shRNA. (F) The Cldn-11 effect on the NICD1 level is dependent on ADAM10. GFP or Cldn-11 overexpressing MC3T3-E1 cells were treated with 10 μM GI254023 (an ADAM10-specific inhibitor) or vehicle for 72 hours prior to immunoblotting using anti-NICD1. (G) *ALP* mRNA levels in GFP or Cldn-11 overexpressing MC3T3-E1 cells in the presence of 10 μM GI254023 or vehicle. Cells were treated with the inhibitor or vehicle for 72 hours prior to RNA extraction for real time PCR. Values (mean ± SEM, n = 4) are fold-change vs. vehicle-treated GFP control. **$P < 0.01$ vs. vehicle-treated GFP control.

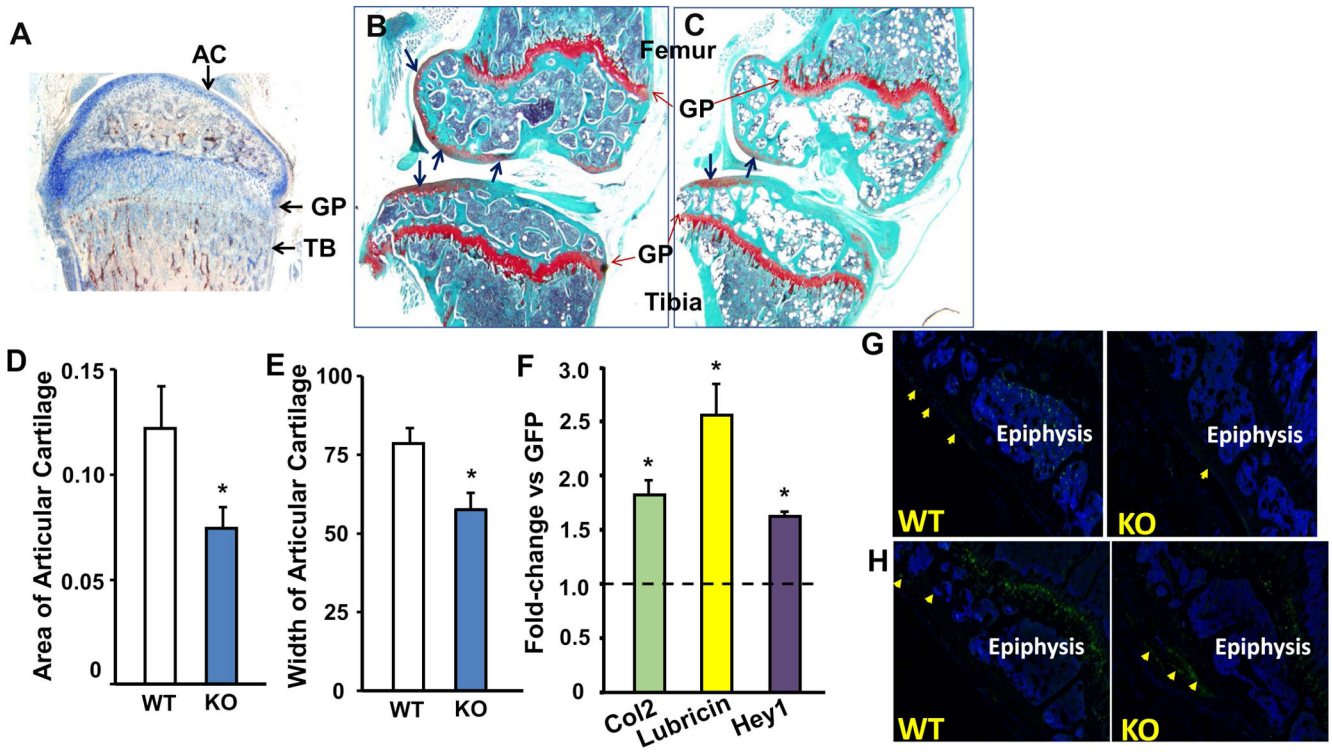

Fig. 10.

Cldn-11 regulates articular cartilage. (A) Immunohistochemical detection of Cldn-11 in chondrocytes of 12-week-old WT mouse. AC, articular cartilage. GP, growth plate. TB. trabecular bone. Black arrows show blue-stained Cldn-11 expression. (B) Safranin-O-stained longitudinal section of a knee joint from a WT mouse. Blue arrows show stained cartilage. (C) Safranin-O-stained longitudinal section of a knee joint from a KO mouse. Blue arrows show stained cartilage. (D) Quantitation of articular cartilage area (mean ± SEM, n = 10–12) in the WT and control mice. *$P < 0.05$ vs. control mice. (E) Quantitation of articular cartilage thickness (mean ± SEM, n = 10–12) in the WT and control mice. *$P < 0.05$ vs. control mice. (F) Immature articular chondrocyte marker (*Col2* and *lubricin*) and Notch target (*Hey1*) mRNA levels in GFP or Cldn-11 overexpressing MC3T3-E1 cells. Values (mean ± SEM, n = 4) are fold-change vs. GFP control. *$P < 0.05$ vs. GFP. (G) Immunofluorescent images of articular cartilage from WT and KO mice showing decreased lubricin expression in the KO cartilage. (H) Immunofluorescent images of articular cartilage from WT and KO mice showing increased Col10 expression in the KO cartilage.